CALORIMETRY FOR SSC DETECTORS

C. Baltay
Columbia University, New York, N.Y. 10027

J. Huston and B.G. Pope
Michigan State University, East Lansing, MI 48824

This report is based on the work of the Calorimetry group and the Jets and Missing E_T group. Participants included A. Abashian, G. Alverson, D. Ayres, C. Baltay, A. Beretwas, R. Blair, G. Brandenberg, J. Butler, B. Cox, J. Ernwein, P. Grannis, H. Iwasaki, L. Jones, D. Judd, J. Huston, H. Kagan, S. Kim, S. Majewski, B. Milliken, S. Linn, B. Oh, R. Panvini, B.G. Pope, S. Protopopescu, J. Linnemann, W. Kienzle, R. Raja, D. Reeder, M. Shibata, T. Sjostrand, W. Smith, D. Stork, G. Theodosiou, D. Underwood, P. Wiesmann, A. White, K. Yasuoka, H. Williams.

I. Introduction

Calorimetry is going to be an important component in most SSC Detectors for measuring energies and angles of both electromagnetic and hadronic particles. Calorimeters already play an important role in detectors at the Sp$\bar{p}$S, TeV I, SLC, and LEP. Their importance will increase at the much higher energies of the SSC since the energy resolution of calorimeters improves with energy as $\sigma/E \sim 1/\sqrt{E}$, while the momentum resolution of magnetic spectrometers deteriorates at high energies as $\sigma/p \sim p$.

At the 1986 Snowmass Summer Study the Calorimetry group concentrated on calorimeters for the large 4π detectors envisioned for the SSC. The "Model A" 4π detector of the 1984 Snowmass Study shown in Fig. 1, served as the starting point. We realized that many of the specialized non-4π detectors may also need calorimetry and that their requirements and parameters could be very different from those of the 4π detectors. Limitations of time and manpower at Snowmass 86 however limited us to the discussions of calorimetry for 4π detectors only.

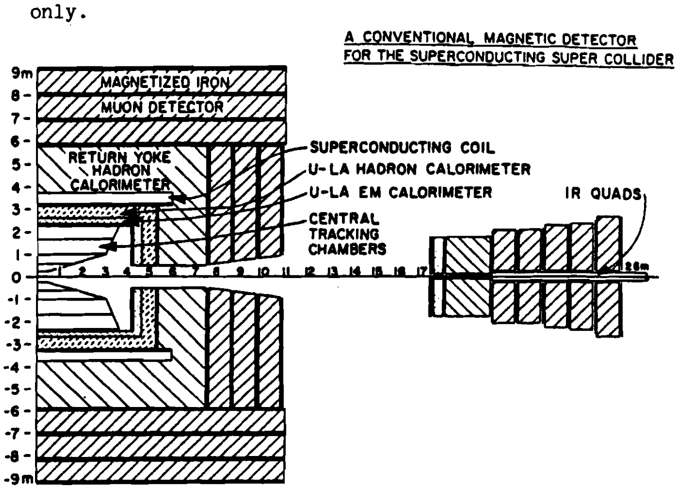

Fig. 1 Snowmass 1984 SCD 4π Detector

II. Desired Parameters of the Calorimeters for the 4π Detector

A. General Philosophy.

The general philosophy followed was to have high quality precision electromagnetic and hadronic calorimetry inside the coil producing the central magnetic field in the detector. However the total thickness of calorimetry required at the SSC energies is so large that the cost of high quality precision calorimetry for the entire thickness is prohibitive. It was therefore envisioned to limit the precision part to a thickness that corresponds to containing about 85% of the energy of a high energy hadronic shower. The remaining 15% tail would be measured by instrumenting the magnet flux returning iron yoke into a relatively inexpensive "tail catcher" calorimeter. All of these calorimeters should contain barrel and end cap regions to cover as much of the full 4π solid angle as possible.

B. Thicknesses Required.

The calorimeter thickness (in units of hadronic absorption lengths λ) to contain hadronic showers as a function of the incident hadron energy is shown in Fig. 2. These curves are based on a parametrization by Gordon and Grannis (Snowmass 1984, p 541). The criteria

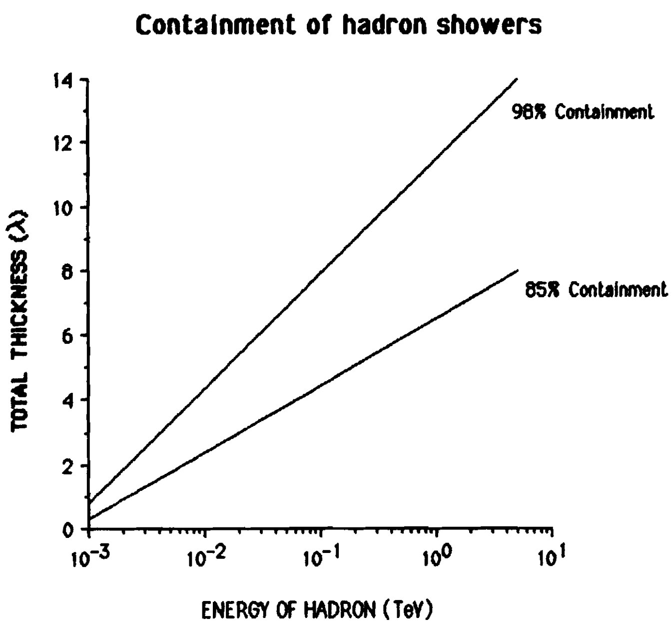

Fig. 2 Containment of Hadronic Showers

used to pick the total depth of the calorimeter was that it contain 98% of the energy of a 1 TeV hadron. From the curves of Fig. 2 this corresponds to ~12 λ. The thickness of the precision calorimeter was chosen to contain 85% of the energy of a 1 TeV hadron, which is ~ 6 λ. There are parametrizations of the energy containment other than Fig. 2 that are somewhat more optimistic. The criteria for choosing the thicknesses described above are based on optimizations of SLC and LEP energies. The consensus was however that the total thickness was appropriate to within ± 2 λ and the thickness of the precision part to ± 1 λ.

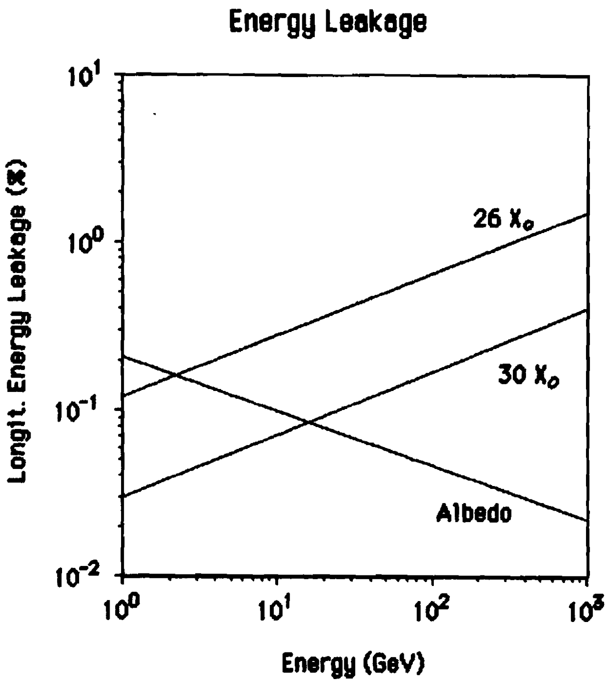

Fig. 3a Energy Dependence of Longitudinal EM Energy Leakage as a Function of Absorber

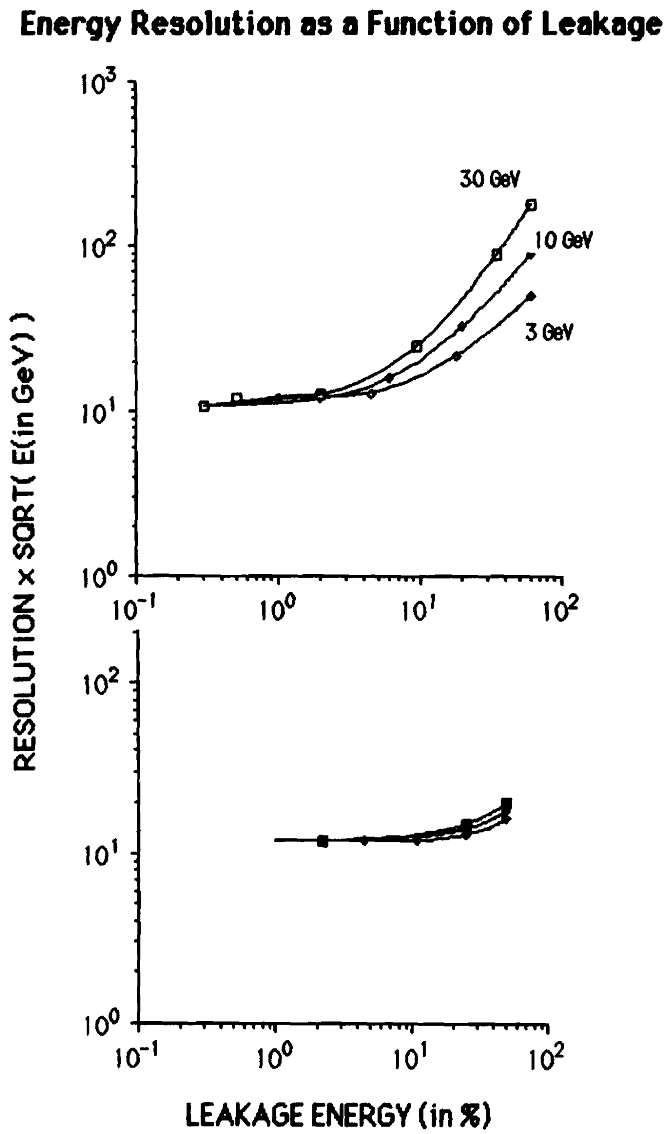

Fig. 3b Energy Resolution as a Function of Leakage Energy.

The thickness of the electromagnetic part of the precision calorimeter was chosen to be 25 radiation lengths on the basis of calculations by T. Kondo and K. Niwa, from the proceedings of Snowmass 84, shown in Fig. 3. The energy leakage out of 25 radiations lengths is less then a few % up to 1 TeV (Fig. 3a). The calculation (Fig. 3b) indicates that a few % leakage does not significantly affect the resolution of an electromagnetic calorimeter of the resolution we are contemplating.

C. Transverse Segmentation.

There was a strong conviction that finely segmented tower geometry was crucial for the high multiplicities expected at the SSC. A number of detailed studies were made investigating the physics capabilities of transverse segmentation of the electromagnetic calorimeter in the range of $\Delta y \times \Delta\phi$ from 0.01 x 0.01 to 0.05 x 0.05. While it was clear that the finer the better, no thresholds or sharp dependences were found to justify any particular segmentation in this range. A segmentation of 0.03 x 0.03 was chosen based on considerations of position resolution. This segmentation corresponds to electromagnetic towers 6 to 8 cm square, which gives enough energy sharing between adjacent towers to give position resolution of the order of 1/10 of the tower size. With coarser segmentation their resolution is expected to deteriorate rapidly. The segmentation in the hadronic part of the precision calorimeter and the hadronic tail catcher was chosen to be $\Delta y \times \Delta\phi = 0.06 \times 0.06$. The main argument for this choice was that a high energy jet should be spread out over many towers, of the order of 5 x 5, to allow study of jet shapes and effective masses.

D. Longitudinal Segmentation.

Similar studies were made to investigate the dependence of the physics capabilities on the number of longitudinal segments into which each tower is divided. The general conclusion was that two longitudinal segments in both of the hadronic sections were sufficient. The electromagnetic section was divided into 3 segments to improve the electron-hadron separation in the calorimeter.

E. Energy Resolution.

The energy resolution of both electrom-magnetic and hadronic calorimeters is usually parametrized as

$$\sigma/E = A/\sqrt{E} + B$$

where the $A/\sqrt{E}$ term is due to sampling fluctuations and B represents the systematic errors due to calibration, stability, etc. The hadronic resolution may also have additional terms as for example C/E, due to uranium noise. As we go to SSC energies the relative contribution of the A term decreases and the importance of B increases. In Table I we list

Table I

1. Electromagnetic Calorimeters

E (GeV)	$1\%/\sqrt{E}$	$10\%/\sqrt{E}$	$20\%/\sqrt{E}$	
1	1%	10%	20%	Constant term B
10	0.3	3	6	~2 to 3% in pre-
50	0.14	1.4	3	sent detectors
100	0.1	1	2	
500	0.04	0.4	0.9	Hope for ~1% at
1000	0.03	0.3	0.6	the SSC

2. Hadronic Calorimeters

E (GeV)	$35\%/\sqrt{E}$	$50\%/\sqrt{E}$	$65\%/\sqrt{E}$	$80\%/\sqrt{E}$	
1	35%	50%	65%	80%	Constant B
10	11	16	21	25	~4 to 6% in
50	5	7	9	11	existing
100	3.5	5	6.5	8	large detec-
500	1.6	2.2	2.9	3.6	tors. Hope
1TeV	1.1	1.6	2.1	2.5	for ~1 to 2%
5TeV	0.5	0.7	0.9	1.1	at the SSC.

At SSC Energies the Constant term B (due to systematics such as calibration and stability) becomes a very important consideration.

contribution of the A term decreases and the importance of B increases. In Table I we list the contribution of the A terms in both electromagnetic and hadronic calorimeters. In present day electromagnetic calorimeters the B term is at best 2 to 3%. One can hope to reduce this term to ~1% in the future. We can see from Table I that with a B term around 1%, the precision afforded by a calorimeter with an A term of $1\%/\sqrt{E}$ is not realized at SSC energies. A $10\%/\sqrt{E}$ is almost as good over most of the energy range. A desired resolution of the electromagnetic calorimeters is therefore chosen to be $(10 \text{ to } 15\%)/\sqrt{E}$.

The constant term in existing large hadronic calorimeters is at best B = 4 to 6%. One hopes to improve this by a factor of 2 in the future. Even then the difference between $35\%/\sqrt{E}$ and $55\%/\sqrt{E}$ at the higher energies is not so large. Thus a precision hadronic calorimeter with resolution in the range $35\%/\sqrt{E}$ and $55\%/\sqrt{E}$ would be desirable.

Another important consideration for hadronic calorimeters is the relative response to electromagnetic and hadronic showers, usually referred to as the e/π ratio.

The basic consequence of $e/\pi \neq 1$ for a hadronic calorimeter is the addition of a constant term to the resolution, of the form discussed earlier. In Figure 4, the value of this constant term is shown as a function of the e/π response (at 10 GeV). If we follow the criteria set earlier (constant term ~2-3%), then the e/π ratio should be $\sim 1 \pm 0.15$.[1]

The dependence of the energy resolution for high energy jets as a function of the e/π ratio and the resolution $\sigma/\sqrt{E}$ for individual

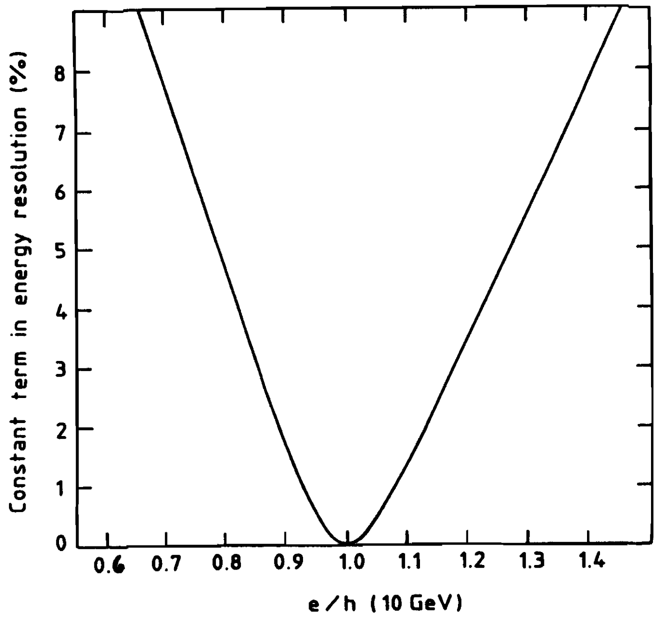

Fig. 4 Variation of the Constant term in Energy Resolution as a Function of e/π.

hadrons is shown in Fig. 5. To keep the jet resolution in the range of 4 to 7% it is important to have an e/π ratio of less than 1.2. It should be noted that the curves of Fig. 5 do not include effects due to the jet defining algorithms, not collecting all of the energy of the jet, or of energy due to tracks not in the jet being mixed in with the jet. These effects will increase the energy resolution for jets somewhat and wash out some of the dependence on e/π and simple hadron resolution.

F. Summary of Parameters.

The desired parameters of the calorimeter for the 4π Detector at the SSC discussed above are summarized in Table II.

III. Results Available from Prototype Calorimeters.

A large number of prototype calorimeters using various radiator materials and readout techniques have been constructed and tested in the past two years in connection with detectors for the SppS, TeV I, SLC, LEP and HERA. The results available from

Table II

4π Calorimeter Parameters

Electromagnetic thickness	$25\ X_0$,	$\sim 1\lambda \pm 5X_0$
Precision Hadronic	5λ	
Total Precision EM + Hadr.	6λ	$\pm 1\lambda$
Hadronic tail catcher	6λ	$\pm 1\lambda$
Total	12λ	$\pm 2\lambda$
Transverse Segmentation		
EM $\Delta y \times \Delta\phi$	.03 x .03	± .01
Hadronic $\Delta y \times \Delta\phi$	.06 x .06	
Tail Catcher $\Delta y \times \Delta\phi$	.06 x .06	
Longtitudonal Segmentation		
EM	3	± 1
Hadronic	2	± 1
Tail Catcher	2	± 1
Electromagnetic Energy Resolution		
	$\sigma/E = \sim 12\%/\sqrt{E}$	± 3%

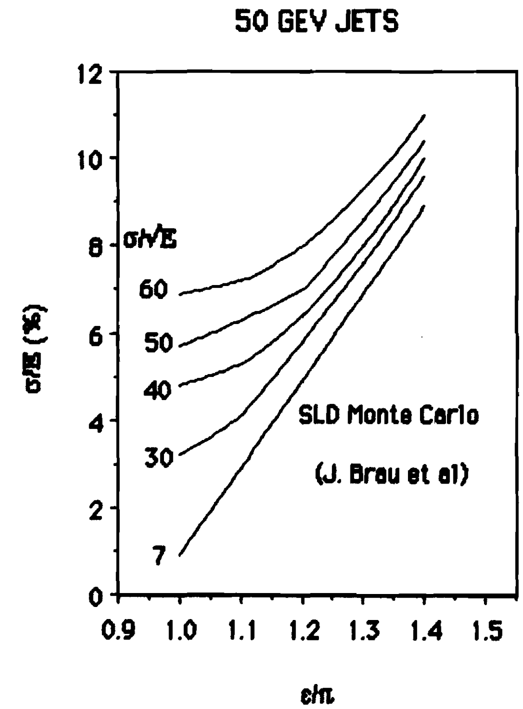

Fig. 5a Energy Resolution as a Function of e/π

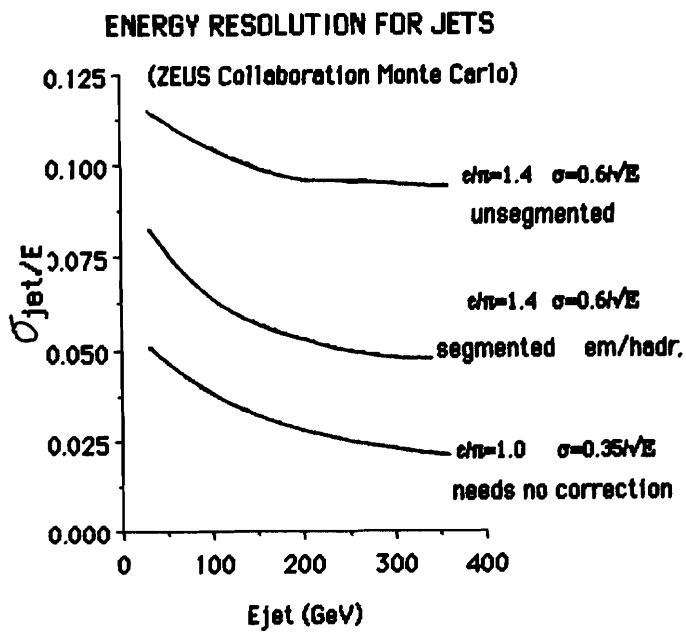

Fig. 5b Energy Resolution for Jets

these tests are summarized in Table III. The e/π ratios and resolutions for single hadrons have been measured in these tests. The last two columns, the resolution for high energy jets, are calculations.

IV. Choice of Calorimeters for the SSC.

A. Possibilities considered.

There was very good agreement that the hadronic tail catcher should consist of the magnetic flux return iron, in the form of 5 cm thick plates, instrumented with gas readout tubes. This technology is now widely used in the new generation of SLC and LEP detectors and needs very little further discussion. Energy resolution of the order of 75%/√E can be expected. To get 6 interaction lengths we need twenty layers with 5 cm Fe plates; with about 3 cm for the gas tubes for each layer the total thickness for this part of the calorimeter will be about 1.6 meters.

The choice for the precision calorimeter inside the coil is much less clear. To get a feeling for physical dimensions a conceptual design was carried out for those technologies listed on Table IV that promise better then 8% resolution on 50 GeV jets. These were uranium radiator with scintillator, liquid argon, gas, or warm liquid (TMP) readout, and lead with liquid argon readout.

B. A conceptual design for the precision electromagnetic and hadronic calorimeter using the various techniques discussed above have been carried out. A rough outline of these designs is as follows:

Table III

Performance of Various Calorimeters based on prototype test results

Radiator/Sample	e/π	σ_{Had}/E	σ_{jet}/E * 50Gev	σ_{jet}/E * 400GeV
U/Scint	1.0	35%/√E	4%	2%
U/Liqu. Ar.	1.1	45%/√E	6%	3%
Pb/Liqu. Ar.	1.25	55%/√E	8%	4%
Fe or Cu/Liqu.Ar.	1.6	60%/√E	14%	9%
Fe/gas	1.6	80%/√E	16%	11%
U/gas	1.0	60%/√E	7%	3-1/2%
U/TMP	?	?	?	?
	±0.1	±5%/√E	±?	±?

*Calculations from SLD & HERA collaborators NOT taking into account errors due to cluster finding, backgrounds, etc.

Design Parameters:
- EM thickness: 25 X.
- EM + Hadronic: 6 λ

Radiators:
- EM: 2mm U or 2 mm Pb
- Hadr.: 6 mm U or 12 mm Pb

Readout:
- Liqu. Ar/G10 boards: 5 mm (2+1+2)
- Liqu. Ar/tiles: 2 mm
- Scintillator - thickness equal to radiator
- Gas tubes: 12 mm

Overhead:
- Liquid Argon Dewars etc.: 40 cm
- Scintillator Phototubes: 30 cm
- Gas readout support struct.: 10 cm
- TMP Liquid vessel + support: 20 cm

TOTAL Calorimeter thickness (in cm)

	Liquid Argon				
	Tiles	G10	TMP	Scintill	Gas
Uranium	125	152	132	139	228
Lead	165	180			

The lead-liquid argon using G10 readout pads and the uranium-gas tube readout were discarded as requiring too much thickness which would excessively drive up the cost of the coil and the iron outside it. We were then left with four possiblities: Uranium with scintillator, liquid argon, or TMP readout and lead with liquid argon readout.

C. A comparison of the various possibilities for the precision calorimeter (electromagnetic and hadronic) is summarized in Table IV. A few detailed comments on this comparison table follow.

Table IV
Comparison of Various Calorimeters

Rad./Sampl.	e/π Ratio	σ_{HAD}/E	σ_{jet}/E* 50 GeV	Thick. for 6 λ (cm.)	Integ. Time (nsec)	Stab. and Calib.	Radiation Hardness
U/Scintill.	1.0	$35\%/\sqrt{E}$	4%	140	15	diff.	marginal
U/Liqu. Ar.	1.1	$45\%/\sqrt{E}$	6%	152	200	good	good
U/gas	1.0	$60\%/\sqrt{E}$	7%	228	50	diff.	O.K.
U/TMP	?	?	?	132	200	good	good
Pb/Liqu. Ar.	1.25	$55\%/\sqrt{E}$	8%	165	200	good	good
Fe, Cu/Liqu. Ar.	1.6	$60\%/\sqrt{E}$	14%		200	good	good
Fe/gas	1.6	$80\%/\sqrt{E}$	16%		50	diff.	O.K.

*NOT including errors due to cluster finding, backgrounds, etc.

1. Readout time problem with Liquid Argon.
   a) Integration time.
   The drift velocity for electrons in pure liquid argon is ~200 nsec/mm. With 1/2% of methane this can be reduced to ~100 nsec/mm. For a minimal liquid argon gap of 2 mm this implies an integration time of at least 200 nsec. At a luminosity of 10^{33} cm^{-2} sec^{-1} this means that on the average 20 events are mixed together in the calorimeter.
   b) Signal Rise Time.
   With specially designed electronics and very short (a few meters at most) leads one can get fast enough signal rise time to measure the time of the energy deposition in a given tower to less then 15 nsec, the time between beam crossings, provided that the energy deposit is more than a few GeV and the tower receives energy from a single event only. With ~20,000 EM and ~5000 hadronic towers most towers will have substantial energy from one event only and can be assigned to the correct beam crossing or event.
   c) The remaining problem then is the occasional towers that get substantial energy from several events. It is not clear at this point whether or not the electronics can tell that this happened. The effect of this energy pileup on the physics is under study.[2,3] For most situations there does not appear to be a severe problem.

2. Scintillator compared with liquid argon for readout of uranium calorimeters.

a) Arguments in favor of Liquid Argon:
i) Liquid Argon is very radiation resistant, and can be used at all angles or radii at the SSC. Scintillators vary in radiation hardness. Acrylic scintillators are damaged by 10^4 Rads, polystyrene can take a few x 10^5 Rads, and a new scintillator SCSN38 has been tested up to 10^6 Rads without serious degradation of performance. The radiation dose expected for a typical calorimeter in a 4π detector at the SSC is shown in Fig. 6. One can see from this figure that above 10° or 20° from the beam direction the scintillators should survive the radiation. However liquid argon is far superior from this point of view.

RADIATION DAMAGE OF SCINTILLATOR

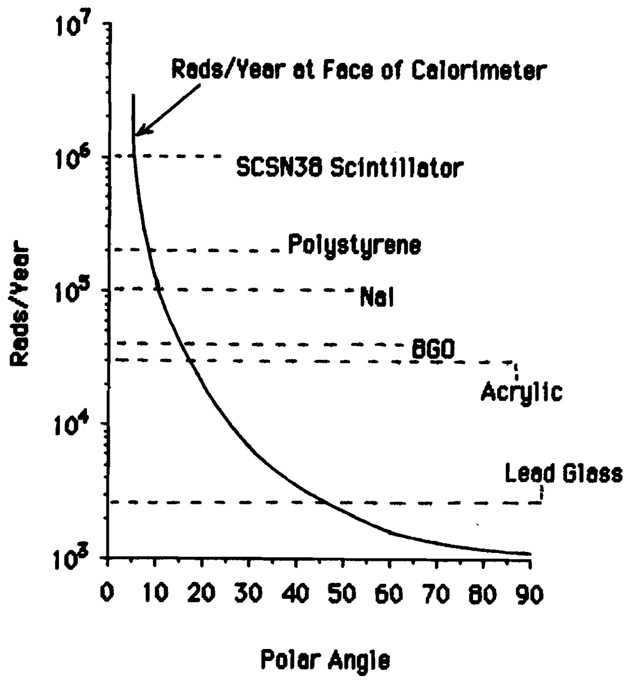

Fig. 6 Radiation Damage of Scintillators. Calculations from the report of B.G. Pope in the PSSC Conclusions (June 1984).

ii) Ease and stability of calibration.
In liquid argon readout there is no gain. The efficiency of the charge collection depends only on the geometry of the plates and gaps. Thus the calibration of the system is very straightforward (there is no need to calibrate each individual tower). Furthermore, once calibrated, the stability of the calibration is excellent. In scintillator the light collection efficiency may vary from tower to tower, as will the response of the phototubes or diodes. Thus every tower will have to be calibrated. And even if calibrated, the efficiencies and gains will vary with time.
iii) Uniform response.
The liquid argon is usually confined in a large vessel and surrounds the radiator plates, so that a uniform response can be expected. With

scintillators one will need wavelength shifter bars or some other form of light guides, which cause cracks that degrade the uniformity of the response.

iv) Finer segmentation is possible with liquid argon readout. The segmentation is probably going to be limited by electronics cost. Because of the need for wavelength shifter bars or some other light guide material, a segmentation finer then $\Delta y \times \Delta\emptyset \sim 0.03 \times 0.03$ seems prohibitive and the number of longitudinal sections is limited to two or at most three.

b) Arguments in favor of scintillator readout.

i) Uranium-scintillator calorimeters have experimentally demonstrated that they are capable of full energy compensation. The experimentally measured hadron energy resolution of $\sigma/E = 35\%/\sqrt{E}$ is the best of any calorimeter built so far.

ii) Short readout time. With some care the scintillators can be read out in ~10 nsec as compared with the 200 nsec integration time of liquid argon. This short readout time of scintillator would allow a separation of events from different beam crossings (the time between beam crossings is about 15 nsec).

A note of caution is necessary here; the very short readout time may not be consistant with collecting all of the energy compensation, some of which is carried by slower neutrons.

iii) The bulky liquid argon and vacuum vessels needed for liquid argon readout causes dead regions near the barrel-end cap overlap region. These dead regions can be considerably reduced in a scintillator calorimeter.

3. Warm Liquid Readout

Organic liquids that can be used at room temperature for calorimeter readout have been pioneered by the UA1 collaboration at CERN. They have considered three liquids with the following properties:

Liquid	Boiling Point	Collection time nsec/2mm gap	Comments
TMS	27°C	80 nsec	Cannot use with U
TMP	122°C	320	UA1 choice
diTMS	151°C	160	

In all of these liquids the output signals are ~1/4 of those in liquid argon. To obtain acceptable electron collection and efficiencies purities of better then 10 parts per billion have to be maintained.

a) Advantages of Warm Liquid readout

i) Warm Liquid readout have most of the good features of liquid argon readout, namely:

Radiation hardness
Ease and stability of calibration
Uniform response
Allows fine segmentation

ii) The big advantage is that warm liquids do not require the liquid argon dewars and the associated cryogenics

b) Problems with Warm Liquids

i) e/π ratio, Hadronic resolution unmeasured

ii) Difficulty of achieving the necessary purity in a large system

iii) Long term stability not demonstrated

iv) Low output signal levels

v) Both TMS and TMP are highly flammable, posing a formidable safety problem.

Hopefully many of these questions will be answered in the near future by the experience of the UA1 collaboration.

4. Comments on Gas Readout for Precision Calorimetry

a) Advantages of gas readout

i) Much easier and cheaper to build than other systems

ii) Requires no cryogenic dewars etc. so it can be more hermetic, with less gaps and cracks in coverage.

iii) Large output signals allows for cheaper electronics per channel. Thus one can afford finer segmentation (i.e. more readout channels) for a fixed electronics cost.

b) Possible problems with gas readout

i) Gas tubes with readout pads require 10 to 12 mm of space per layer, instead of 2 mm of liquid argon. In a fine grained EM & precision hadronic calorimeter with 100 or so layers this can add 50 to 100 cm of radial space. This increases the size (and thus the cost) of the rest of the detector outside of the calorimeter.

ii) Somewhat poorer energy resolution then liquid argon:

$20\%/\sqrt{E}$ electromagnetic instead of $10\%/\sqrt{E}$

$60\%/\sqrt{E}$ hadronic instead of 35 to $55\%/\sqrt{E}$

iii) Difficulty of high precision calibration and stability

iv) Long term survival in high radiation environment not demonstrated.

v) Linearity at high energies not demonstrated.

5. Comparison of Uranium-Liquid Argon with Lead-Liquid Argon.

a) Electromagnetic energy resolution is similar

b) e/π ratio and hadronic energy resolution somewhat worse with lead (see Tables III and IV)

c) Density of Lead/Liquid Argon/Tile readout is within 10% of Uranium/Liquid Argon/G10 readout (Tile readout with uranium requires a prohibitive amount of machining).

d) Lead has no uranium noise

e) Uranium is very difficult to obtain and to work with

f) Cost comparison: Uranium is more expensive then lead, and G10 readout boards are expensive. A very rough cost estimate for an SSC 4π calorimeter, with $25X_0$ electromagnetic and 5 λ precision hadronic section indicate that uranium-liquid argon system might cost 50M$ compared with 30M$ for a lead-liquid argon system (these numbers do not include electronics which should be the same for both).

V. The Physics of Missing E_T Measurement

The discovery of new phenomena involving production of non-interacting particles requires of calorimetry the ability to measure missing transverse momentum. Background to these new types of events comes mainly from multijet events in which one or more jets are lost or mismeasured. The mismeasurement can be due to either physics causes (neutrinos carrying away jet momentum) or instrumental causes. In the calorimetery group the impact of several instrumental effects was considered, including hermiticity, resolution and pileup.

The natural scale to compare the calorimetric measurement of missing E_T with is that due to neutrino production in jets. The level of neutrino production in jets has been studied by Iwasaki. In Table V the neutrino multiplicity is given for different flavors of 1 TeV/c jets.

Table V. Neutrino multiplicity (= Mν)
1 TeV < Pt (jet) < 1.1 TeV

	mean Mν	Mν = 0	Mν ≠ 0
light q (u,d,s)	0.06	0.96	0.04
c	0.24	0.79	0.21
b	0.73	0.50	0.50
t	1.31	0.27	0.73
gluon	0.36	0.82	0.18

Light quark jets contain neutrinos with only a 4% probability whereas heavy quark jets have probabilities for neutrinos varying from 21% for c quarks to 73% for t quarks. It is interesting that gluon jets have similar tendencies for neutrino production as heavy quark jets. This is due to the relatively copious[4] production of heavy quarks in high p_T gluon jets.

The fraction of p_T taken by neutrinos in 1 TeV/c jets is shown in Table VI. As expected, there are significant differences between light quark jets (only ~1% of jet p_T taken on average) and heavy quark jets (for t quarks 11% of the p_T is lost). The distributions are plotted in Figure 7. It is especially interesting to note the broadness of the distribution for t quark jets. The above quantities were studied as a function of p_T (for t quark jets) with no strong dependence being found.

Table VI. Pt of neutrino
1 TeV < Pt (jet) < 1.1 TeV
x = Pt (ν's)/Pt (parton)

	for Mν ≠ 0		for all sample	
	$\bar{x}$	σ_x	$\bar{x}$	σ_x
light q(u,d,s)	2.2×10^{-2}	2.2×10^{-2}	1.1×10^{-3}	6.8×10^{-3}
c	9.1×10^{-2}	1.0×10^{-1}	1.9×10^{-2}	5.9×10^{-2}
b	9.8×10^{-2}	9.4×10^{-2}	4.9×10^{-2}	8.3×10^{-2}
t	1.5×10^{-1}	1.7×10^{-1}	1.1×10^{-1}	1.6×10^{-1}
gluon	5.7×10^{-2}	7.7×10^{-2}	1.1×10^{-2}	4.0×10^{-2}

Iwasaki, Milliken, Protopopescu and Raja have conducted a study (see report these proceedings) on the effects of missing and dead material on the hermiticity of calorimetry. The effects of cracks in the calorimetry on the measurement of missing E_T can be estimated by constructing a quality factor

$$QF = \int d\eta \, d\phi \, (\Delta E/E)$$

Quite reasonably the severity of a crack is proportional to its η and φ coverage and to the proportional energy loss that takes place inside it. This is somewhat of a simplification as this energy

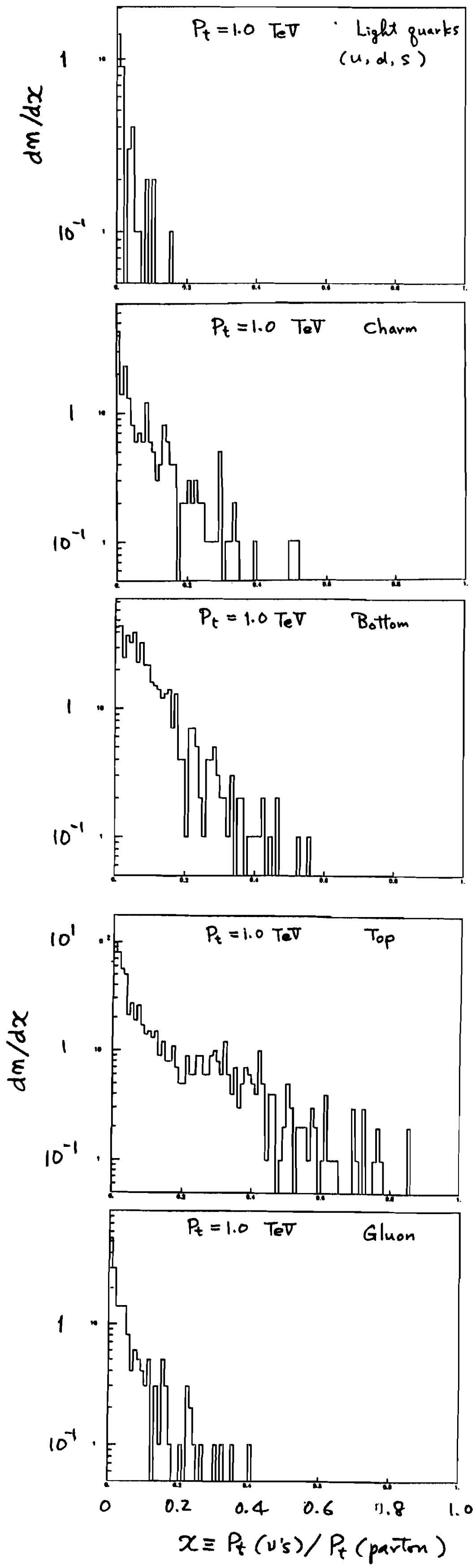

Fig. 7 Missing P_T due to Neutrinos

loss (for small energy losses) can be partially compensated by looking at the surrounding calorimetry. A complete understanding of the severity of each crack, unfortunately would require the generation of a large number (10^6?) of Monte Carlo events with full shower simulations. Until this computer power is available, quality factors of this type can give a reasonable idea of the relative severity of different cracks.

One crack that is unavoidable is one to allow the beam to pass through. The effect of beam holes of 0.5°, 1° and 2° was studied (by the above group) using ISAJET 5.22. It differs from the version used in Snowmass '84 in that initial state radiation is allowed. The effect, as seen in Figure 8, is to greatly enhance the contribution of beam holes to missing E_T. The crossover between the neutrino contribution and that due to a 0.5° beam hole is likely to be at 100 GeV/c rather than about 60 GeV/c.

The effect gets larger for higher p_T jets due to the increased Q^2 of the interaction. This result emphasizes, even more than in Snowmass '84, the need for calorimetry down to very small angles with respect to the beam.

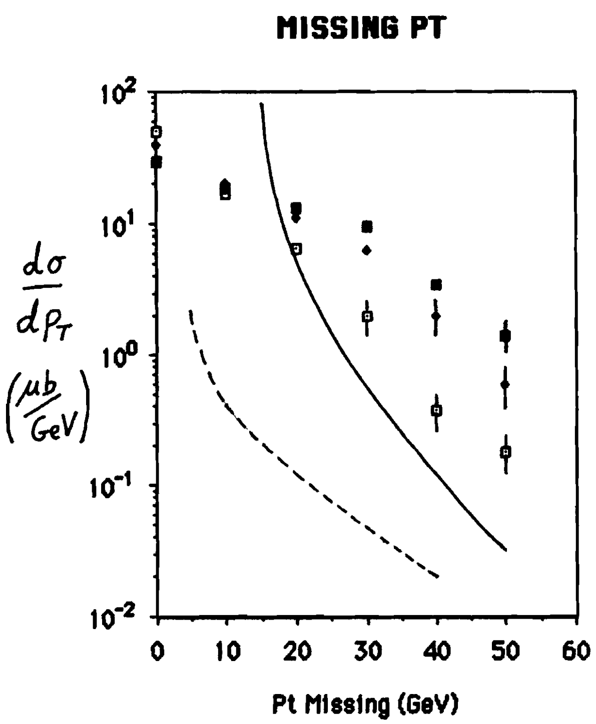

Figure 8. Missing p_t (Isajet 5.22) requiring $30<p_t<100$ GeV: solid squares below 2°, solid diamonds below 1° and open squares below 0.5°. The solid line is the missing p_t below 1.5° calculated at Snowmass '84 (Isajet 4.0). The dashed line is missing p_t contribution from neutrinos.

Finite energy and angle resolutions give contributions towards the missing E_T resolution of a calorimeter of the form $\sigma \lesssim \sqrt{\Sigma E_T}$. With $\sigma_{EM} = 1.5 \times \sqrt{E}$ and $\Delta\theta \times \Delta\phi = 5° \times 17°$ and $\sigma_{HAD} = .80 \times \sqrt{E}$ and $(\Delta\theta \times \Delta\phi)_{HAD} = 15° \times 18°$, UA-1 has observed[5] $\lesssim 0.7$. In Snowmass '84 a study with $\sigma_{EM} = .15 \times \sqrt{E}$ $\sigma_{HAD} = 0.35 \times \sqrt{E}$ and $\sigma_y = \sigma_x = 2$ cm found $\lesssim 0.3$. Reasonable energy and angular resolutions for calorimetry will have only a modest effect on the missing E_T cross sections that are due to the finite rapidity coverage of the detector ($\eta = \pm 5.4$, for example).

The high event rate at the SSC implies that any calorimeter not employing heroic efforts to minimize its integration time will feel the impact of a large number of events. This pileup will create a "physics noise" for any calorimetric measurement. This was studied in detail by two groups: Alverson and Huston,[2] Yamashita and Kondo.[3]

A liquid argon calorimeter, seemingly the detector of choice for the SSC so far, requires a charge collection time on the order of at least 200 ns. Employing bipolar pulse shaping leads to an effective integration time of about twice that. The distribution of E_T per cell for this integration time (and .06 x .06 cells) is shown in Figure 9.

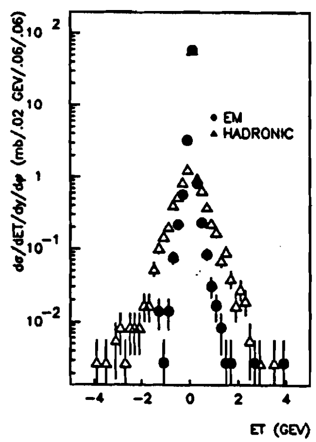

Fig. 9 E_T distributions per cell

The distributions are symmetric with respect to zero, naturally, because of the bipolar pulse shaping. The standard deviations are 90 MeV for electromagnetic energy and 220 MeV for hadronic energy. (The standard deviations are somewhat different for the Yamashita and Kondo study as they smeared the energy over several cells using a shower shape parameterization.) It's not quite fair to treat this as a gaussian noise as the distribution is not very gaussian (90% of the events are in the 0-200 MeV/c bin and 85% of the time the cells are empty.

The standard deviations scale with the square root of both the integration time and the cell area. This is reasonable since the multiplicity and energy deposited scales linearly with these quantities and so the standard deviations should scale as the square root.

In Figure 10, the missing E_T cross section is compared for "standard SSC events" for one beam crossing and for an integration time of 400 ns. Both the mean and standard deviation increase significantly. (Both also scale as the square root of the integration time.)

Note that in addition to resolution effects these distributions also contain contributions from neutrinos and particles going down the beam hole ($\theta<0.5°$). For example, in Figure 11, the missing E_T cross section is shown for an integration time of 400 ns for a calorimeter with perfect resolution but keeping a beam hole of $\theta = 0.5°$.

Since these "cross sections" are so large they can cause a significant background for physics

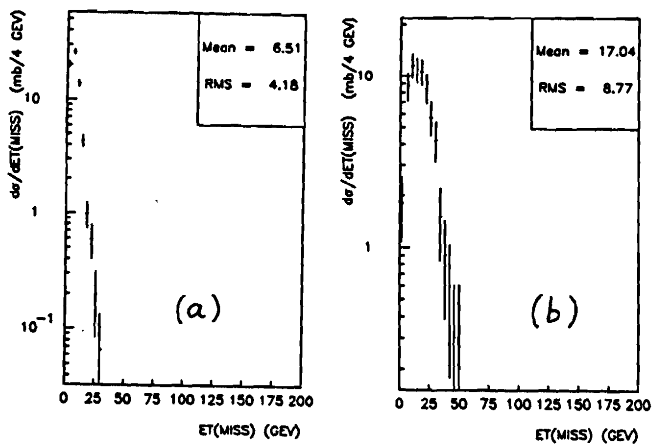

Fig. 10 (a) $d\sigma/d^{miss}_{ET}$ for one beam crossing

(b) $d\sigma/d^{miss}_{ET}$ for t_d = 200 nsec

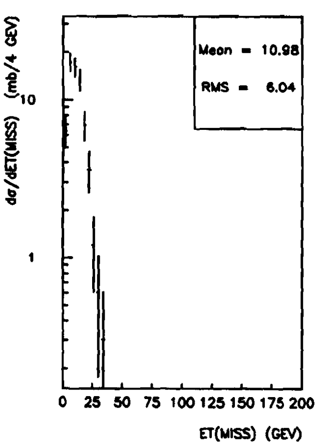

Figure 11 $d\sigma/dE_T^{miss}$ for "perfect resolution"

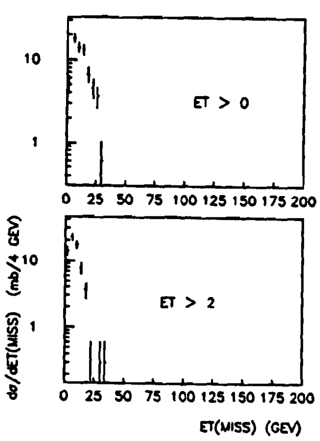

Fig. 12 $d\sigma/dE_T^{miss}$ with energy cuts

processes with moderate amounts of missing E_T. One effective timing cut that can be applied is simply to require that the E_T in each cell be positive., This is shown in Figure 12 along with the requirement that E_T/cell > + 2 GeV/c.

One form of pileup that is unavoidable at the SSC is that due to multiple interactions in the same beam crossing. With an average of 1.4 interactions per crossing, if a bunch crossing contains one interaction, there is a 74% chance that there is more than one. Stork has performed a study (these proceedings) showing the utility of instrumenting the beam region (250 microradian, neutral calorimeter system in neutral interaction beam dump + hadron calorimeters placed along beam pipe in vertical bend sections) to tag multiple interactions. The measured energy is shown in Figure 13 for one, two and three interactions.

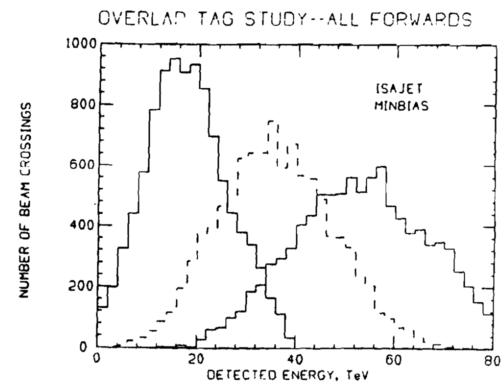

Fig. 13 Response of the calorimeter system for one, two, and three minimum bias interactions.

Of course, the environment that these detectors would face would be very hostile. The calorimetry would have to be very fast (<10 ns) and very radiation hard. Perhaps a sampling calorimeter using BaF_2 could be used. Recent tests have shown little radiation damage with an exposure of up to 10^8 rads (of photons). Because of the natural spread of the energy distributions being measured, however, the energy resolution can be very coarse.

V. Comment on Future R & D on Calorimeters.

We will learn a lot about calorimetry from the large collider detectors now under construction:

Uranium/Liquid Argon	DØ
Lead/Liquid Argon	SLD
Uranium/scintillator	ZEUS
Uranium/gas	L3
Uranium/TMP	UA1
Lead/gas tubes	ALEPH
Fe/gas tube (Hadronic Tail Catcher)	ALEPH, DELPHI, SLC, OPAL

With the exception of the Fe/gas tubes for the Hadronic Tail Catcher, the lack of agreement on the technology of choice is striking. Each major detector is pursuing a different approach. This diversity of approach is to the advantage from the point of view of the SSC in that a wide range of technologies will be very thoroughly tested in the next few years. This should produce a wealth of information on which to base the design for calorimeters at the SSC.

There are two areas in which the requirements of the SSC are more stringent then those for the detectors above. These are the need for high radiation resistance and the need for extremely high data rates. In these two areas R & D directed specifically toward the SSC will be required.

VI. General Conclusions

1. High quality calorimetry for a 4π detector for the SSC seems feasible at the full 10^{33} design luminosity, with the following features:
   a. Finely segmented projective tower geometry, with $\Delta y \times \Delta\phi \sim 0.03 \times 0.03$.
   b. Good electromagnetic and hadronic resolution: $\sigma_{em}/\sqrt{E} \sim (10 \text{ to } 15\%)/\sqrt{E}$, $\sigma_{had}/\sqrt{E} \sim (35 \text{ to } 55\%)/\sqrt{E}$.
   c. Similar response to e, γ, and hadrons: e/π ratio from 1.0 to 1.2.
   d. Hermetic 4π coverage down to 1° from the beam direction.

2. Several techniques are feasible, with different tradeoffs between advantages and problems.
   a. Uranium or Lead radiators with Liquid Argon readout are the present day favorites.
   b. Uranium with warm liquid or scintillator readout could become the first choice, depending on progress with these readout techniques in the next few years.
   c. Iron plates with gas tube readout is the technique of choice for the Hadronic Tail Catcher calorimeter.

3. An SSC Calorimeter (~25 radiation lengths thick electromagnetic, ~6 interaction lengths thick precision electromagnetic plus hadronic, with a ~6 interaction length thick hadronic tail catcher) is a reasonable extrapolation of the calorimeters in the detectors now under construction at SppS, TeV I, SLC, LEP and HERA.

References

1. On the Energy Resolution of Uranium and Other Hadron Calorimeters, Richard Wigmans, CERN/EP 86-141 (September 1986).

2. Estimation of Background Noise in LAr Detectors due to Pileup, G.O. Alverson and J. Huston, these proceedings.

3. Physics Noise to Calorimetry at SSC, A. Yamashita and K. Kondo, these proceedings.

4. A. Mueller and P. Nason, Nucl. Phys. B266, (1986) 265.

5. J.P. Mendiburu, private communication.

6. D. Anderson and S. Majewski, Summary Report of the PSSC Discussion Group Meetings, (1984) 191.